Journal of Thermal Analysis and Calorimetry (2023) 148:12725–12737
https://doi.org/10.1007/s10973-023-12577-4

Kinetic study and effect of flash pyrolysis temperature of kraft lignin on the yield of aromatic compounds

Gislane Pinho de Oliveira[1,2,3] · Lorena Araújo de Melo Siqueira[1] · Guilherme Quintela Calixto[1,3] · Dulce Maria de Araújo Melo[1,4] · Marcus Antonio de Freitas Melo[1,3] · Alexandre Santos Pimenta[5] · Renata Martins Braga[1,3,5]

Received: 8 September 2022 / Accepted: 17 September 2023 / Published online: 18 October 2023

Abstract

The growth in global energy demand and the urge to reduce CO_2 emission make renewable sources viable alternatives to replace fossil fuels and petrochemicals. Black liquor, a by-product of pulp industry, has been mostly burned to generate energy. Nevertheless, its pyrolysis is an alternative valorization route for obtaining valuable aromatics. The present study aims the energetic characterization of kraft lignin, evaluation of the kinetics of commercial alkaline lignin as a standard model, and the study of the renewable aromatics yield obtained from flash pyrolysis of kraft lignin at 400, 500 and 600 °C. The kinetic study shows an increasing apparent activation energy up to 760 °C, with a maximum value of 338.2 kJ mol^{-1}. The reaction order greater than one for 35–840 °C reinforces the bimolecular mechanism degradation. The main pyrolysis products were phenolics and aromatics with methoxy groups. The highest amount of phenolics, toluene, and *p*-xylene was obtained at 600 °C. Results show that lignin has low energetic potential for thermochemical processes due to the low content of volatiles (45.64%) and ash (21.6%), and low calorific value (15 MJ kg^{-1}). Despite low volatile content, the results show kraft lignin is a renewable alternative source with potential to generate building blocks.

Keywords Kinetic study · Kraft lignin · Flash pyrolysis · Renewable aromatics

Introduction

The increasing global energy demand and the urge to reduce CO_2 emission make renewable sources viable alternatives to replace fossil fuels and petrochemicals. Large volumes of black liquor, composed mainly of inorganic reagent residues and lignin dissolved after the digestion step in the kraft process, are generated by the pulp industries for the manufacture of paper, additives, construction material, and cellulosic ethanol production [1]. The black liquor is the main by-product of the pulp industry, being a renewable resource with potential for valuable aromatic compounds production [2]. However, its main application has been the generation of energy through burning, contributing 64.13% of all energy generated in the Brazilian industry of planted tree sector [3] and 3% in the national energy matrix [4], with only 2% of the bleach being used commercially to obtain high value-added chemicals [5].

Lignin is a complex and irregular polymer formed by the polymerization of H (*p*-hydroxyphenyl), G (guaiacyl) and S (syringyl) units derived from three monolignols, *p*-coumaryl

✉ Renata Martins Braga
renata.braga@ufrn.br

Gislane Pinho de Oliveira
gislaneoliveira@gmail.com

Dulce Maria de Araújo Melo
daraujomelo@gmail.com

1 Environmental Technology Laboratory, Federal University of Rio Grande do Norte, S/N - Lagoa Nova, Natal, RN 59072-970, Brazil

2 Environmental Engineering, Federal University of Maranhão, MA-140, km 04, Balsas, MA 65800-000, Brazil

3 Postgraduate Program in Chemical Engineering, Federal University of Rio Grande do Norte, S/N - Lagoa Nova, Natal, RN 59072-970, Brazil

4 Institute of Chemistry, Federal University of Rio Grande do Norte, S/N - Lagoa Nova, Natal, RN 59072-970, Brazil

5 Escola Agrícola de Jundiaí, Federal University of Rio Grande do Norte, RN-160 - km 03 - Distrito de Jundiaí, Macaíba, RN 59280-000, Brazil

alcohol, coniferyl alcohol and sinapyl alcohol, respectively, which differ in the amount of methoxy groups attached to the phenolic core (Fig. 1) [6]. The bonds between the units are predominantly of ether type (> 66%); among these, the β-O-4 ether bond is the most abundant, accounting for 45–60% of the connectivity between monomers, followed by 5–5 (3–20%) and β-5 (3–12%) C–C bond types. The S/H/G ratio depends on the plant species. Softwood lignin contains G units only, while hardwood lignin, like those obtained from eucalyptus, is composed of both G and S units (Fig. 1). Herbaceous lignin is composed of all three units, showing H fraction < 5% [6]. Lignin is more abundant in softwood biomasses (27–30%) than hardwood (20–25%) and grasses (5–20%) [7].

The chemical complexity, recalcitrance, non-uniform structure, inherent reactivity, different types of inter-unit bonds, predisposition to form condensed structure, low selectivity and the presence of various organic and inorganic impurities make the processing of kraft lignin a challenge [8, 9], which motivates several studies in order to provide strategies for its valorization.

Compared to holocellulose, lignin has higher carbon content and lower oxygen content, in addition to having a highly functionalized nature [10]. Lignin is the largest natural source of renewable aromatic compounds, making it attractive to produce biofuels and bioproducts such as benzene, toluene, ethylbenzene, xylene (BTEX) and phenols, which are mostly of petrochemical origin. Recent researches obtained monophenolic compounds from lignin in birch sawdust [11], phenols from hardwood, softwood, and herbaceous lignins [12] and aromatics from lignin residue [13]. Previous researches on kinetics decomposition of lignin estimated the apparent energy activation either without determining the reaction order and the pre-exponential factor [14, 15] or setting a first-order reaction to determine the pre-exponential factor [16], revealing a lack of studies that determine the three kinetics parameters: apparent energy activation, reaction order and pre-exponential factor.

Lignin valorization through pyrolysis to obtain bioproducts contributes to the bioeconomy by partially replacing the fossil carbon source with a renewable one. It also promotes the circular economy by using an undervalued by-product that belongs to the low carbon economy. The pyrolysis of lignin is a better alternative when compared to its combustion. Lignin combustion releases CO_2 emissions—a greenhouse gas—while pyrolysis provides a solution with a cost-effective approach [17] for renewable aromatics obtention from dry biomass that reduces the environmental impact caused by greenhouse gas emitted by its burning.

Thus, considering the large abundance of lignin, its availability to the market as an industrial by-product derived from the kraft process and the large-scale use of the eucalyptus plant for pulp and paper production, the present work aims to evaluate the decomposition kinetics

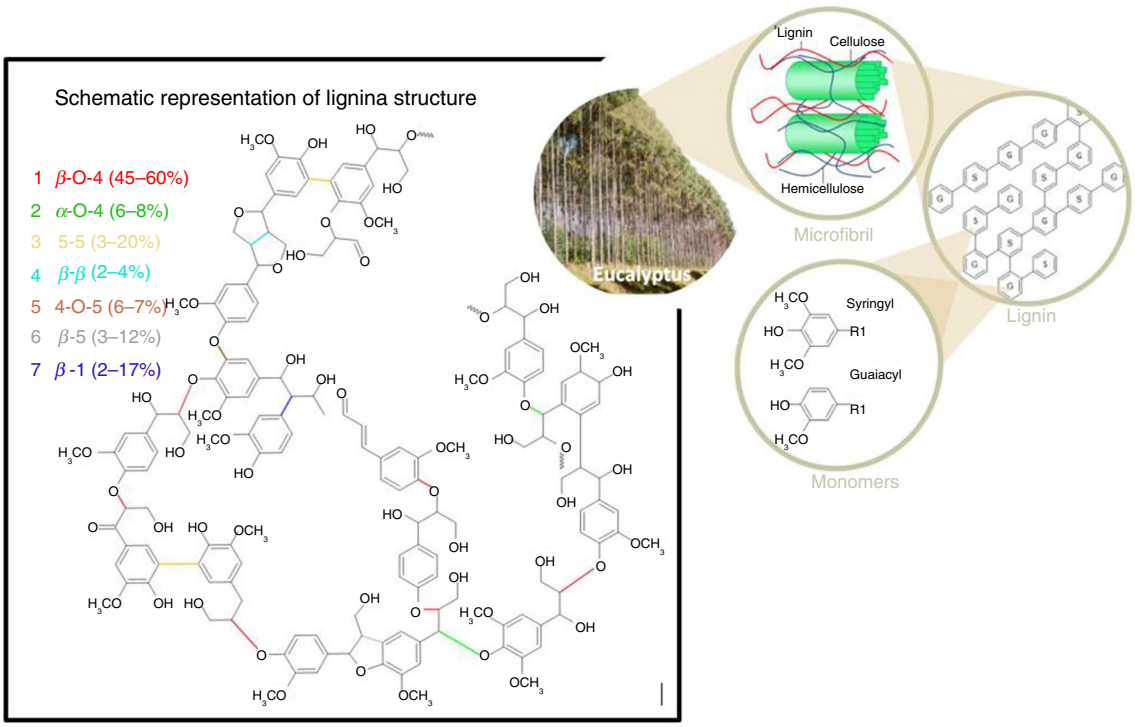

Fig. 1 Diagram of the lignin structure, highlighting the monomers that form the lignin obtained from eucalyptus

of commercial alkaline lignin as a standard model and the influence of flash pyrolysis temperature of kraft lignin to obtain renewable mono aromatics such as BTX and phenols.

Materials and methods

Energetic characterization of kraft lignin

The kraft lignin obtained from pulping wood clones (*Eucalyptus urophylla* x *Eucalyptus grandis*) was supplied by an industrial unit of cellulose, located in Jacareí—São Paulo. The material was dried in oven at 100 °C for 16 h, followed by sieving with selection of particles between − 100 + 140# (0.149 mm) for energy characterization and analytical pyrolysis.

The immediate chemical analysis was determined following the procedures of the American Society for Testing and Materials (ASTM) to determine the moisture content (ASTM E871-82), ash content (ASTM E1755-01) and volatile material content (VM) (ASTM E897 and E872). The fixed carbon content (FC) was calculated by difference. The superior calorific value (SCV) was estimated according to the model of Cordero et al. [18] following the correlation between the immediate analysis and the superior calorific value using the results of the immediate analysis through Eq. 1.

$$\mathrm{SCV} = 354.3\ (\mathrm{FC}) + 170.8\ (\mathrm{VM})\ (\mathrm{MJ\ kg^{-1}}) \tag{1}$$

Elemental analysis was performed on the PerkinElmer 2400 Series II CHNS/O Analyzer, using the combustion method to convert the elements to single gases (CO_2, H_2O, and N_2). The oxygen content was calculated by difference using Eq. 2.

$$\%\mathrm{O} = 100 - \%\mathrm{C} - \%\mathrm{H} - \%\mathrm{N} - \%\mathrm{S} \tag{2}$$

Thermogravimetric analysis (TG/DTG) of kraft lignin was performed on a Shimadzu Q500 TGA balance, from room temperature to 900 °C with heating rate of 10 °C $\mathrm{min^{-1}}$ and 50 mL $\mathrm{min^{-1}}$ of N_2 (99.999%) using 15 mg of the biomass. Thermogravimetric analysis of commercial lignin sample (alkali lignin from Sigma-Aldrich, CAS Number 8068-05-1) was also performed as a reference standard using approximately 6 mg at heating rates of 10, 20 and 30 °C $\mathrm{min^{-1}}$, from room temperature to 1000 °C. According to the manufacturer, alkali lignin is a brown or black powder with 47–51% carbon, 5.04% hydrogen, 3.37% sulfur, 5.4% sodium and approximately 5% moisture, with similar characteristics to kraft lignin extracted from wood.

Kinetic study

The kinetic study of commercial lignin (alkali lignin from Sigma-Aldrich, CAS Number 8068-05-1) decomposition was developed using the isoconversional Flynn–Wall–Ozawa (FWO) integral model using thermogravimetric data at the heating rates of 10, 20 and 30 °C $\mathrm{min^{-1}}$. The studied ranges were selected by evaluating the main mass loss observed in the deconvolution of the DTG curve assuming Gaussian distribution.

The pyrolytic degradation mechanism of biomass can be considered as a one-step global reaction in which the solid biomass degrades into volatile products and biochar. The kinetics of the reaction of solids in a one-step process can be described by Eq. 3.

$$\frac{\mathrm{d}\alpha}{\mathrm{d}t} = A\mathrm{e}^{\left(-\frac{\mathrm{E_a}}{\mathrm{RT}}\right)} f(\alpha) \tag{3}$$

where $f(\alpha)$ is the reaction model assumed $f(\alpha) = (1-\alpha)^{\mathrm{n}}$, α is the conversion, R is the universal gas constant, and E_a is the apparent activation energy.

The ash-free residue normalized conversion during pyrolysis is calculated according to Eq. 4.

$$\alpha = \frac{m_\mathrm{i} - m}{m_\mathrm{i} - m_\mathrm{f}} \tag{4}$$

where m_i, m e m_f represent the initial, instantaneous and final mass, respectively.

After integrating Eq. 3, at constant heating rate, $\beta = \frac{\mathrm{d}T}{\mathrm{d}t}$, Eq. 5 is obtained:

$$g(\alpha) = \int_0^\alpha \frac{\mathrm{d}\alpha}{f(\alpha)} = \frac{A}{\beta}\int_{T0}^{T} \mathrm{e}\left(-\tfrac{E_\mathrm{a}}{RT}\right)\mathrm{d}T = \frac{AE}{\beta R}.p\left(-\frac{E_\mathrm{a}}{RT}\right) \tag{5}$$

Since the conversion is low for low temperatures, the lower limit of the integral can be simplified to $T_0 = 0$ [19]. The function $p\left(-\frac{E_\mathrm{a}}{RT}\right)$ can be simplified using the Doyle approximation, Eq. 6 [20].

$$\log p\left(-\frac{E_\mathrm{a}}{RT}\right) \approx -2.315 + 0.457\left(-\frac{E_\mathrm{a}}{RT}\right) \tag{6}$$

Isoconversional methods consider that the reaction model $(f(\alpha))$ is constant for each conversion (α_i) of a given heating rate (β_i). Based on these considerations, Flynn–Wall–Ozawa (FWO) proposed a method using the Doyle approximation, Eq. 7 [20]

$$\log\left(\beta_\mathrm{i}\right) \approx \log\left(\frac{A_\alpha E_{\mathrm{a}_\alpha}}{g(\alpha)R}\right) - 2.315 - 0.457\left(\frac{E_{\mathrm{a}_\alpha}}{RT_{\alpha_\mathrm{i}}}\right) \tag{7}$$

Apparent activation energy E_a(kJ mol^{-1}) is obtained from the slope of the linear regression of log (β_i) versus $\frac{1000}{T_{\alpha_i}}$. The data evaluation and fitting were done by minimization of the root sum squared (RSS), Eq. 8, where N is the number of experimental data.

$$\mathrm{RSS} = \sum_{i=0}^{i=N} \left[\alpha_i^{\mathrm{exp}} - \alpha_i^{\mathrm{calc}}\right] \quad (8)$$

The relative deviation was calculated according to Eq. 9.

$$\mathrm{error}\ (\%) = 100\left(\frac{\sqrt{\frac{\mathrm{RSS}^2}{N}}}{\alpha_{\mathrm{exp}}^{\mathrm{max}}}\right) \quad (9)$$

Analytical flash pyrolysis

The analytical pyrolysis of kraft lignin was performed in a CDS Py-5200 HPR from CDS Analytical (Oxford-PA) to evaluate the pyrolysis products at 400, 500, and 600 °C, using heating rate of 10 °C ms^{-1} and nitrogen (99.999%) as carrier and purge gas. The sample (1 mg) was inserted between the top and bottom of quartz wool in a quartz tube (25.38 mm × 1.75 mm ID) and heated by a resistively platinum filament positioned around the tube. After thermal decomposition, the vapors were dragged through He (99.999%) 50 mL min^{-1} and subsequently desorbed in a Tenax trap heated from 30 to 300 °C for 4 min. The desorbed vapors were transferred through a transfer line heated at 300 °C, injected in split mode 1:50 into a gas chromatograph (VARIAN 3900) coupled to a mass spectrometer (VARIAN 3800) and separated on a ZB-5 MS chromatographic column (60 m × 0.25 mm 0.25 µL) using 1 mL min^{-1} of He (99.999%) as the carrier gas. The GC/MS column-programmed temperature was 40 °C for 4 min, followed by heating at 10 °C min^{-1} to 280 °C, remaining at this temperature for 14 min. The spectra of the chromatographic peaks, resulting from pyrolysis, were identified through the commercial NIST library, being considered identified when the spectral similarity is greater than 85%.

Results and discussion

Energetic characterization of kraft lignin

The energetic potential of biomass is measured by its calorific value, given by the amount of energy released per unit mass or volume of the fuel when it is fully combusted. The energy content is directly associated with low moisture and ash content, which comprises the non-combustible part of the biomass, and high volatile material and fixed carbon content, which concentrates the chemical energy of the material.

The energetic characterization of kraft lignin is shown in Table 1. The high ash content of the kraft lignin (21.60 ± 2.28%) is a result of the chemical reagents used in the pulping process, such as NaOH and Na_2S, which adds an inorganic sodium fraction in its composition. Despite the high ash content, this material presents high fixed carbon content. The low volatile content, when compared to lignocellulosic biomass, is due to its polyaromatic composition, thermally stable and with high lignin content since it is a lignin concentrate.

Biomasses with high carbon and hydrogen contents have higher heat capacity due to the energy released by these elements in the combustion reaction [21]. The sulfur found in kraft lignin is a consequence of the lignin extraction method, which by using sodium sulfide (Na_2S) in the kraft process introduces thiol groups in the side chains of lignin. Despite presenting low content (1.7%), sulfur is undesirable because it can cause corrosion in equipment and emission of SO_x into the atmosphere during its thermal degradation.

The decomposition of kraft lignin and alkali lignin (Sigma-Aldrich) occurs gradually within a wide temperature range (150–900 °C), according to Fig. 2, showing high thermal stability. The kraft delignification method, whose intense alkaline treatment promotes severe degradation and repolymerization reactions, leads to a highly condensed material with high thermal stability that contains low amounts of residual β-O-4 bonds [10], which are the weakest ether bonds present in the lignin structure and easily broken at 250–350 °C [22]. Despite undergoing a severe process, the studied kraft lignin showed maximum peak decomposition at lower temperature (310 °C) than lignins obtained from Klason (405 °C) and Organosolv (396 °C) methods [15].

The initial stage of both lignins (kraft and alkaline lignins) decomposition profile is attributed to water evaporation, dehydration reactions and the release of some low molecular weight volatile organic constituents, which generates a loss of about 11% for both lignins. This result agrees

Table 1 Energetic characterization of kraft lignin

Immediate chemical analysis	
Moisture/%	12.44 ± 0.36
Ash/%	21.60 ± 2.28
Volatile content/%	45.64 ± 4.21
Fixed carbon[a]/%	20.32 ± 4.80
Elemental analysis	
$CH_{1.07}N_{0.01}S_{0.01}O_{0.38}$	
Superior calorific value/MJ kg^{-1}	15.0

[a]Calculated by difference

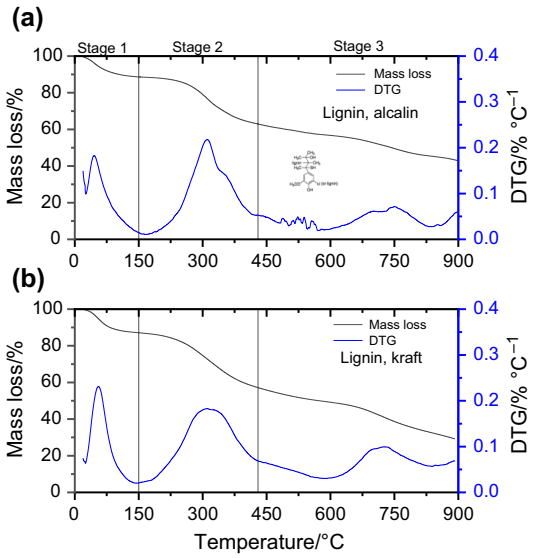

Fig. 2 Thermogravimetric curves (TG/DTG) of **a** alkaline lignin (Sigma-Aldrich), **b** kraft lignin (from industrial unit)

with the previous one obtained by the immediate analysis (Table 2).

A second event occurs between 150 and 430 °C presenting a maximum mass loss peak at 310 °C. In this range, a mass loss of 25.61% and 26.18% is observed for kraft lignin and alkaline lignin, respectively, forming a great amount of volatiles. The volatiles are released due to the partial decomposition of the aromatic structure, composed by three-dimensional, amorphous and branched macromolecules (phenolic hydroxyls, carbonyl groups and benzylic hydroxyls) [15, 23, 24]. Phenolic compounds containing aromatic ring, alkyl and hydroxyl groups, such as guaiacyl, syringyl and phenols with 2-methoxy-4-alkyl substituted radicals, are predominantly released at this stage, reflecting the characteristics of the lignin structure [25]. During this stage the aromatic methoxy groups are stable [26].

The mass loss of approximately 28 and 21% in stage 3, for both kraft and alkali lignin, respectively, may be associated with demethoxylation reactions.

The formation of coke and polycyclic aromatic hydrocarbons begins around 400–450 °C and at temperatures above 500 °C decomposition, and condensation reactions of aromatic rings are predominant, resulting in charcoal as the main product [27]. Above 700 °C the primary pyrolysis reactions of lignin cease completely, while the primary products undergo secondary degradation reactions such as dehydration, decarboxylation and demethylation, and radical rearrangement, producing more gases such as CO, CH_4 and H_2 [28]. At the end of the analysis (900 °C), a residual mass of 29% and 43% was observed for kraft and alkaline lignin, respectively, attributed to the ash content and the fixed carbon.

Kinetic study

Figure 3 presents the deconvolution of the DTG curve at a heating rate of 10 °C min^{-1} assuming Gaussian distribution. The overlap of peaks observed in the DTG curve for the regions 2, 3 and 4 suggests that the degradation of alkaline lignin (Sigma-Aldrich) occurs according to a multi-reaction kinetics. According to Fig. 3, one can indicate a degradation mechanism involving seven reactions that correspond to the degradation of the lignin structure.

Based on Fig. 3, five decomposition ranges were defined, for which the isoconversional FWO model was applied: 35–175 °C, 175–410 °C, 620–760 °C, 660–840 °C, 858–1000 °C. Figure 4 shows the linear regression of the FWO model for conversions between 0.05 and 0.9. The R^2 values for each conversion are shown in Table 3.

The average value of the apparent activation energies (E_a) obtained by FWO method (Fig. 5) was 50.6, 179.2, 338.2, 253.5 and 94.8 kJ mol^{-1} for ranges 1, 2, 3, 4 and 5, respectively. For ranges 1, 2 and 5, between conversions 0.2–0.8,

Table 2 Apparent activation energy (kJ mol^{-1}) and R^2 obtained by the FWO method

α (%)	35–175 °C		175–410 °C		620–760 °C		660–840 °C		858–1000 °C	
	E_a	R^2	E_a	R^2	E_a	R^2	E_a	R^2	E_a	R^2
5	55.9	0.999	98.4	0.993	419. 6	0.981	354.7	0.882	89.5	0.804
10	54.1	0.999	135.2	0.994	389.6	0.964	368.9	0.907	91.5	0.812
20	51.0	1.000	173.8	0.996	372.9	0.915	349.1	0.797	94.4	0.821
30	50.0	1.000	191.7	0.996	367.0	0.867	313	0.760	96.1	0.834
40	49.8	1.000	197.8	0.997	366.1	0.826	274.4	0.785	97.3	0.843
50	50. 5	1.000	196.8	0.996	352.1	0.783	242.3	0.838	97.8	0.850
60	50.9	1.000	192.2	0.994	319.1	0.763	217.3	0.859	97.5	0.854
70	50.6	1.000	195.2	0.990	290.8	0.794	186.5	0.838	96.1	0.855
80	49.7	1.000	201.4	0.987	259.6	0.831	136.2	0.793	94.6	0.853
90	43.8	0.996	209.74	0.975	242.8	0.868	92.6	0.748	93.1	0.849
E_a	50.6		179.2		338.2		253.5		94.8	

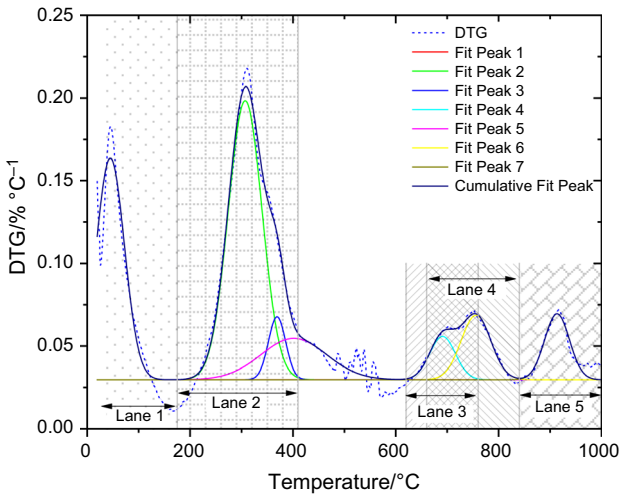

Fig. 3 Deconvolution assuming Gaussian distribution of the DTG curve of alkaline lignin (Sigma-Aldrich) at 10 °C min^{-1}

a maximum variation from the mean of the E value for a given conversion was 1.9%, 12.4% and 3.2%, respectively, suggesting a single-step decomposition. For ranges 3 and 4, the maximum variation is 23.7% and 63.7%, respectively. This suggests that the decomposition mechanism in these ranges occurs following several steps involving parallel, competitive or consecutive reactions. This agrees with what is observed in Fig. 3.

The FWO model showed a good fit to the experimental data for ranges 1 and 2, since the R^2 values were all greater than 0.975 (Table 2). For ranges 3, 4 and 5 the proposed model presented R^2 values higher than 0.748 and therefore does not present an adequate fit, which may be an indication of a change in the reaction mechanism, with a reaction function $f(\alpha)$ that became dependent on conversion or heating rate.

Wang et al. [15] found a similar apparent activation energy $E_a = 139.7$ kJ mol^{-1} for range 2, which corresponds to the breaking of β-O-4 bonds.

The models that best fit the ranges studied are shown in Table 3 and Fig. 6. The pre-exponential factor represents the frequency with which collisions occur between the reactant molecules [29], being expressively higher for ranges 2, 3 and 4.

The reaction order greater than 1 reinforces the bimolecular mechanism of β–O–4 bond degradation, according to mechanism iv of Fig. 7 [30], whose values can also be explained due to the condensed structure of kraft lignin. Three possible pathways for the pyrolytic degradation mechanism of lignin (Fig. 7) have been proposed: (i) C_β–O bond homolysis ($E_d = 221.4$ kJ mol^{-1}), (ii) C_α–C_β bond homolysis ($E_d = 259.3$ kJ mol^{-1}) and (iii) concerted C_β–O decomposition ($E_d = 264.4$ kJ mol^{-1}) [31]. These mechanisms, in turn, consider only unimolecular decomposition of a β-O-4-type lignin model dimer. On the other hand, lignin and the intermediates, radicals and products of its pyrolysis coexist in the

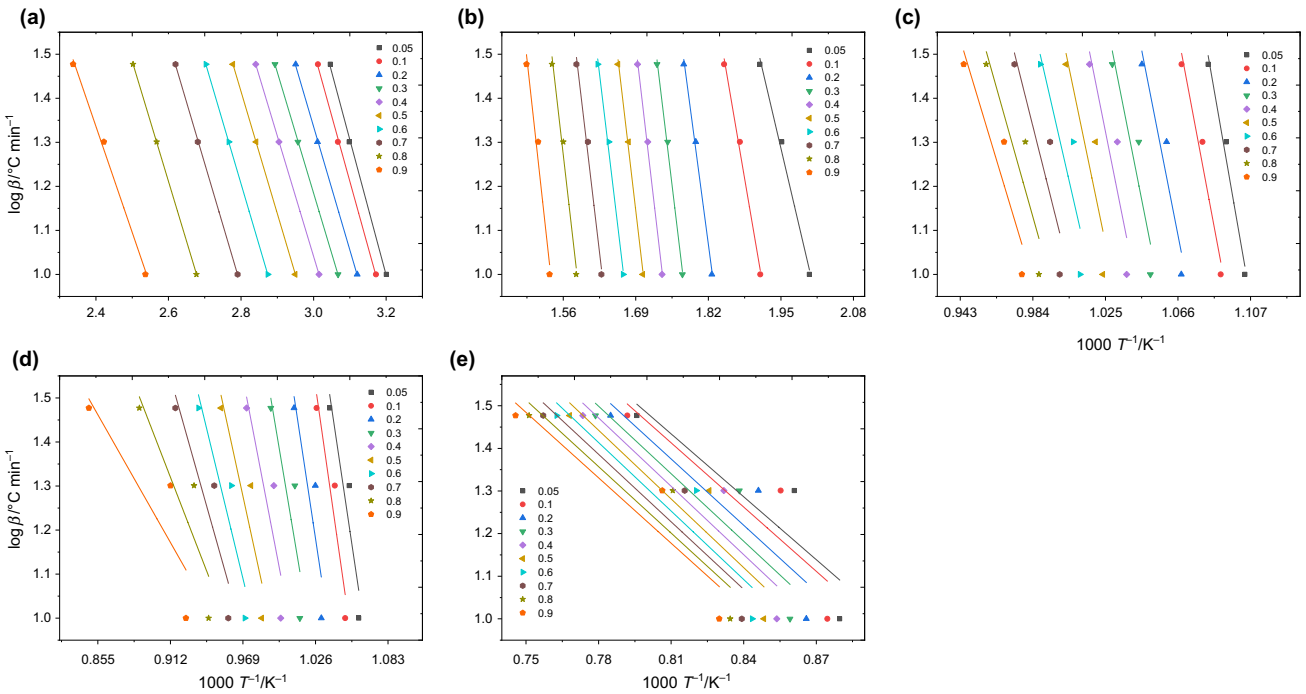

Fig. 4 FWO plot at different conversions for the ranges **a** 1: 35–175 °C, **b** 2: 175–410 °C, **c** 3: 620–760 °C, **d** 4: 660–840 °C, **e** 5: 858–1000 °C of alkaline lignin (Sigma-Aldrich)

Table 3 Kinetic model for the ranges 1: 35–175 °C, 2: 175–410 °C, 3: 620–760 °C, 4: 660–840 °C and 5: 858–1000 °C of Sigma-Aldrich kraft lignin

Range	Kinetic model	Error
1: 35–175 °C	$\frac{d\alpha}{dt} = 5.2 \cdot 10^{7} e^{\left(-\frac{50610}{RT}\right)} (1-\alpha)^{2.5}$	3.2%
2: 175–410 °C	$\frac{d\alpha}{dt} = 7.5 \cdot 10^{15} e^{\left(-\frac{179230}{RT}\right)} (1-\alpha)^{2.9}$	10.4%
3: 620–760 °C	$\frac{d\alpha}{dt} = 6.3 \cdot 10^{17} e^{\left(-\frac{338240}{RT}\right)} (1-\alpha)^{2}$	7.2%
4: 660–840 °C	$\frac{d\alpha}{dt} = 4.2 \cdot 10^{12} e^{\left(-\frac{253500}{RT}\right)} (1-\alpha)^{2}$	5.3%
5: 858–1000 °C	$\frac{d\alpha}{dt} = 2.3 \cdot 10^{3} e^{\left(-\frac{94790}{RT}\right)} (1-\alpha)^{0.15}$	4.0%

reaction medium, allowing complex intermolecular interactions. Then, hydrogen abstraction mechanism takes place through bimolecular reactions between lignin molecules and homolytic radicals, especially phenolic ones (mechanism iv of Fig. 7). In this case, the required dissociation energy (E_d) for decarbonylation, decarboxylation, dehydration and tautomerization reactions is reduced [30].

The proposed kinetic models (Table 3) present satisfactory and similar behavior to that observed experimentally, as shown in Fig. 6. Ranges 2, 3 and 4, in which parallel, competitive or consecutive reactions occur, presented theoretical curves with trends that diverge more from the experimental curves because global reaction kinetics was considered leading to higher relative errors.

Analytical flash pyrolysis

The compounds resulting from flash pyrolysis of kraft lignin were mainly monoaromatic products, phenols, methoxylated phenols and oxygenated compounds of lower molecular mass, containing between 1 and 4 carbon atoms (C1–C4). The identified products correlated well with the structure of lignin, formed through the decomposition of its precursor polymers (H, G and S) by breaking β-O-4, α-O-4 and C–C bonds, then producing a large amount of phenolic structures [27]. The formation of phenolic compounds and low molecular weight volatile species is explained by chain reactions with cleavage of side chains such as $–OCH_3$ and –OH in the aromatic ring [25].

The kraft lignin obtained from eucalyptus, a hardwood lignin which is formed from units G and S (Fig. 1), shows a great diversity and abundance in structure of side chains, resulting in the wide range of derivatives as the main products of pyrolysis [25].

Lignin contains alkyl aryl ether (β-O-4) linkage as a major bond (Fig. 1), representing about 60% of the total polymeric bonds for this molecule. This type of bond is more reactive than the C–C bond, playing a key role in primary pyrolysis.

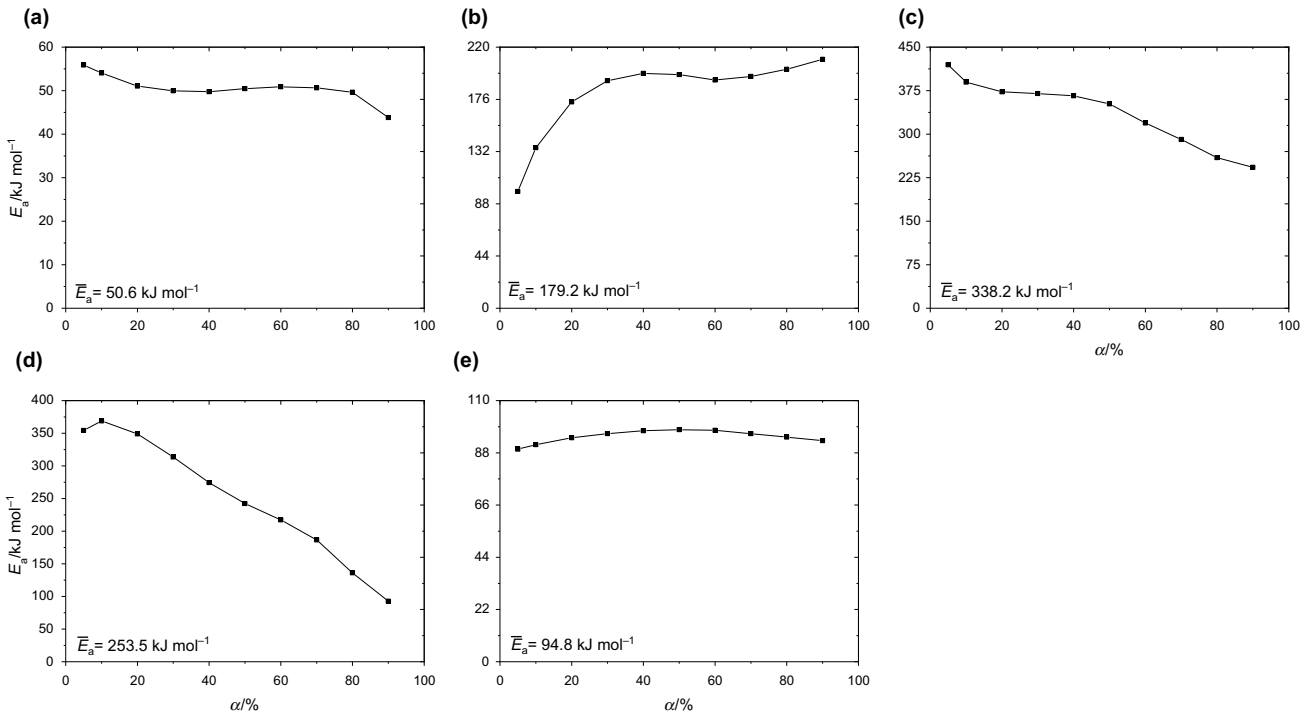

Fig. 5 Activation energy estimated by FWO method for the ranges **a** 1: 35–175 °C, **b** 2: 175–410 °C, **c** 3: 620–760 °C, **d** 4: 660–840 °C, **e** 5: 858–1000 °C of Sigma-Aldrich kraft lignin

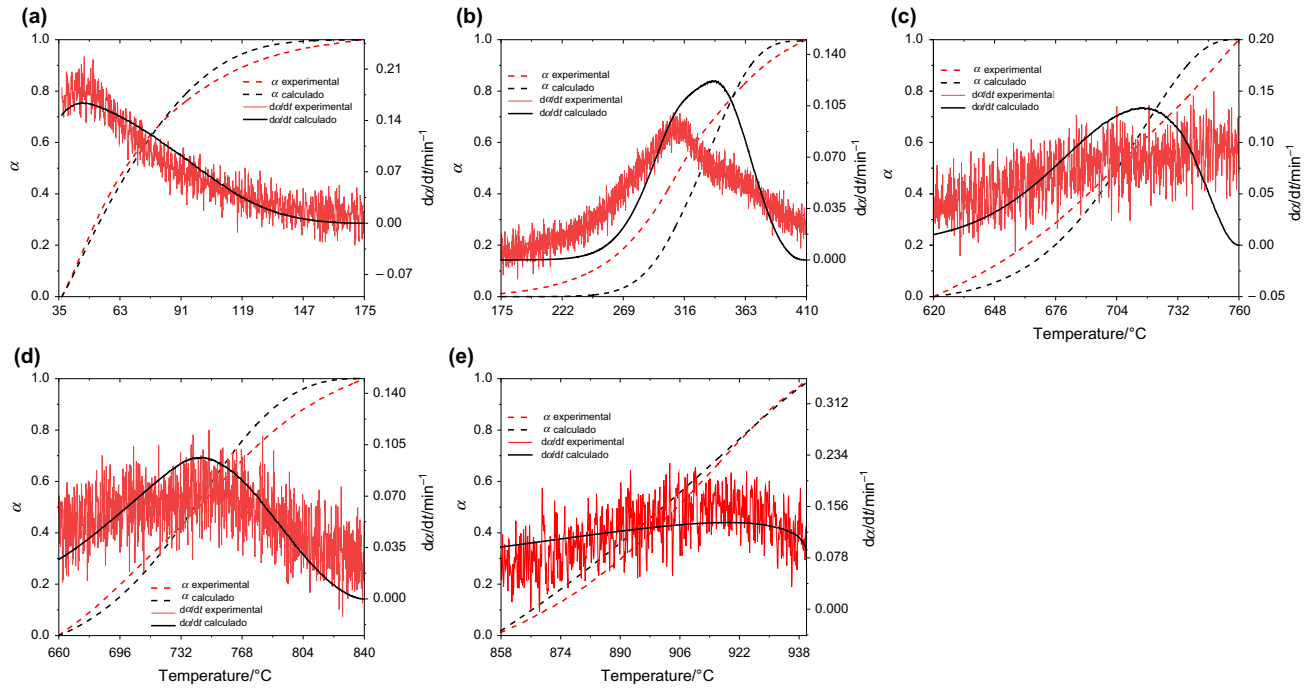

Fig. 6 Experimental and calculated curves of dα/dt at a heating rate of 10 °C min^{-1} for the ranges **a** 1: 35–175 °C, **b** 2: 175–410 °C, **c** 3: 620–760 °C, **d** 4: 660–840 °C, **e** 5: 858–1000 °C of Sigma-Aldrich kraft lignin

The chromatograms of kraft lignin flash pyrolysis at 400, 500 and 600 °C are presented in Fig. 8, and the list of products is identified in Table 4. The %area was calculated excluding the unidentified compounds. Although the peak with a retention time of 13.56 min has one of the highest intensities, it could not be identified because spectral similarity was lower than 85% when compared to commercial NIST library. This peak could be associated with biphenyl or other polycyclic aromatics.

A large amount of phenolic and aromatic compounds generated through thermal degradation, as well as other lower molecular weight compounds such as ketones and sulfides, are obtained at these different temperatures.

Another aspect observed is the progressive increase of phenols, toluene, and p-xylene as the pyrolysis temperature increases, as presented in Fig. 9. The yield of pyrolysis products increased with increasing temperature, and this result can be explained by the volatile release range found in the thermogravimetric analysis, which goes from 180 to 900 °C, i.e., at 600 °C there is a greater degradation of the kraft lignin mass than at 400 and 500 °C.

The main G- and S-type products obtained at the 3 different pyrolysis temperatures are: 1,2-dimethoxybenzene, 2-methoxy-4-methylphenol (4-methyl guaiacyl), 2,6-dimethoxyphenol (siringyl), 2,3-dimethoxytoluene, 5-methyl-1,2,3-trimethoxy benzene, 1,2,4-trimethoxybenzene, 3,4,5-trimethoxybenzaldehyde, 1,2-dimethoxy-4-(2-methoxyethenyl)benzene. Among these compounds, 2-methoxy-4-methylphenol was the product identified with the highest %area. The main product obtained from H-type was 3-methylphenol.

Compared to S-type compounds, G compounds are the predominant primary products of hardwood lignin pyrolysis. One possible pathway for the formation of G and S is the cleavage of the aryl–alkyl–aryl bond, represented by number 7 in Fig. 1, in parallel with the abstraction of the H^+ proton from the phenoxy group (C_6H_5O–), forming hydroxylphenolic [32]. Another way to obtain it is by directly breaking the β-O-4 bond [31] or by eliminating the (R1) group (Fig. 1). Although hardwood lignin is formed by S and G units in similar proportions [33], a greater amount of G-type products was observed compared to S. The percentage of S progressively reduces with increasing temperature until it is no longer detected at 600 °C, while the percentage of G decreases slightly from 400 °C to 500 °C and increases again at 600 °C as the production of phenols and cresols increases. This phenomenon can be explained due to the demethoxylation reactions that gradually transform S into G by O–CH_3 bond homolysis which decomposes to produce phenol, cresol and catechol as the temperature increases above 400 °C [25, 34].

In the range of 400–450 °C, the C–C bond of the side chains starts breaking leading to the formation of monomers with saturated alkyl side chains [26]. Saturated alkyl side chain G derivatives, such as 4-methylguaiacyl (2-methoxy-4-methylphenol) and 4-ethylguaiacyl

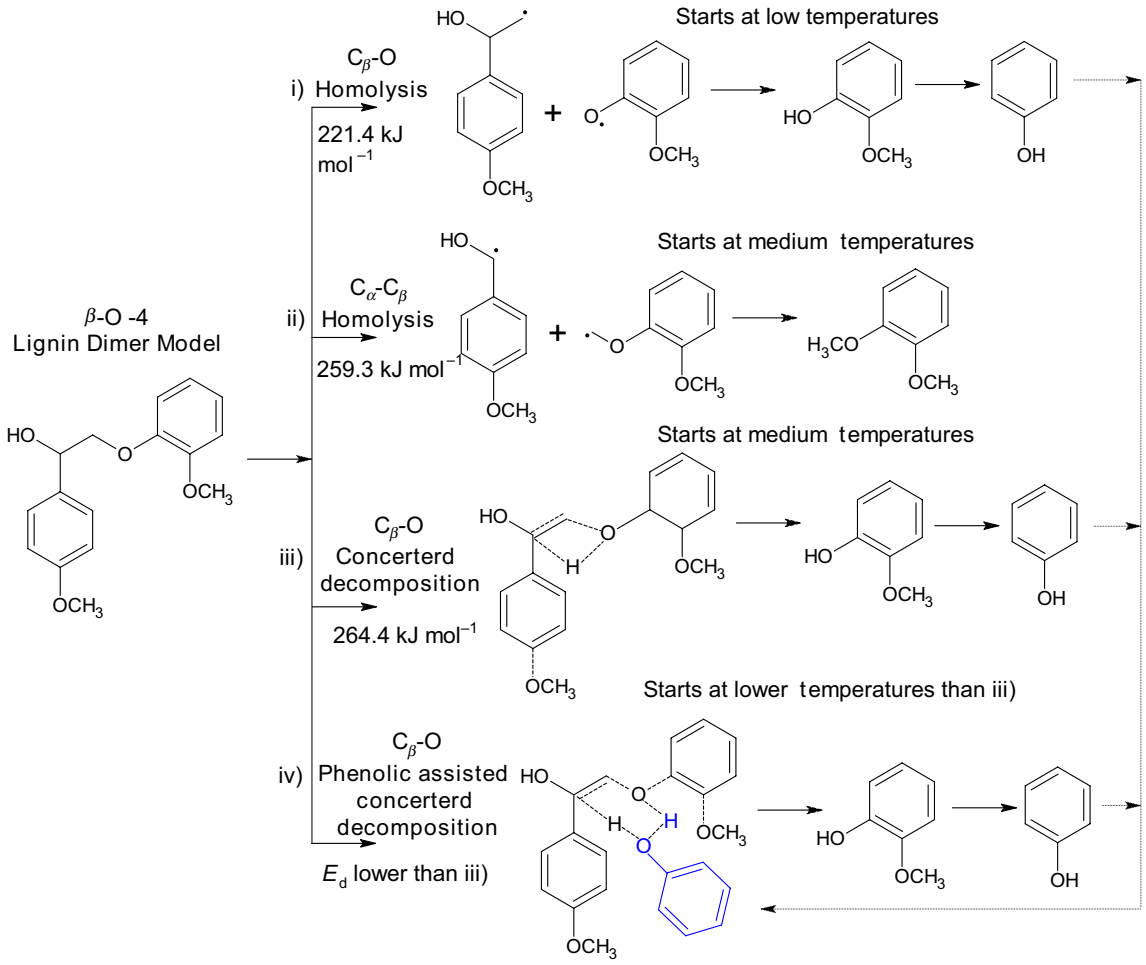

Fig. 7 Pyrolysis mechanism of lignin dimer as a simplified model of the lignin molecule. *Source*: Adapted from Chen et al. [31]

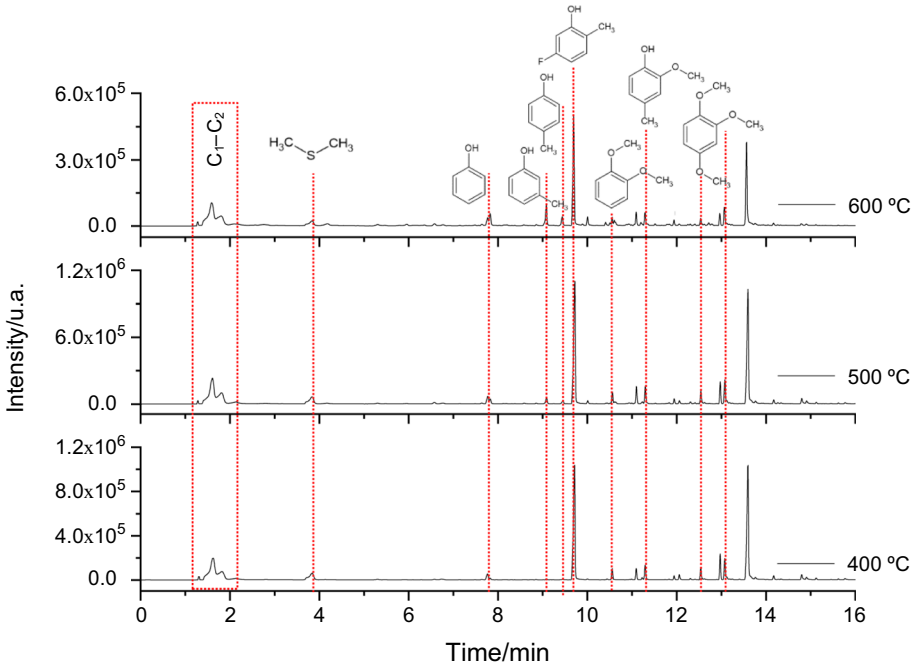

Fig. 8 Flash pyrolysis chromatograms of kraft lignin at 400, 500 and 600 °C

Table 4 Compounds obtained from flash pyrolysis of kraft lignin at 400, 500 and 600 °C

Compound	Chemical formula	Area[a]/%		
		400 °C	500 °C	600 °C
(C1–C4)	–	22.90	21.90	26.77
Acetic anhydride	($C_4H_6O_3$)	–	12.02	–
Dimethyl disulfide	($C_2H_6S_2$)	6.41	5.50	4.70
Toluene	(C_7H_8)		0.66	1.68
p-xylene	(C_8H_{10})	–	0.55	2.24
2-Hepten-4-one	($C_7H_{12}O$)	–	0.19	–
3-Methyl-2-cyclopenten-1-one	(C_6H_8O)	0.14	0.25	–
Dimethyl trisulfide	($C_2H_6S_3$)	2.78	–	–
Diethyl thioether	($C_4H_{10}S$)	–	1.24	–
Phenol	(C_6H_6O)	–	0.43	–
2,3-Dimethyl-2-cyclopenten-1-one	($C_7H_{10}O$)	0.13	0.21	–
3-Methylphenol	(C_7H_8O)	0.26	1.72	6.88
4-Methylphenol	(C_7H_8O)	–	0.93	2.86
5-Fluoro-2-methylaniline	(C_7H_8FN)	42.41	36.53	34.19
2.6-Dimethylphenol	($C_8H_{10}O$)	–	0.62	–
2-Ethyl phenol	($C_8H_{10}O$)	–	–	0.77
1,2-Dimethoxybenzene	($C_8H_{10}O_2$)	2.47	1.97	1.34
2,4-Dimethylphenol	($C_8H_{10}O$)	–	–	2,65
2-Methoxy-4-methylphenol	($C_8H_{10}O_2$)	2.95	6.97	7.12
2-Ethyl-5-methylphenol	($C_9H_{12}O$)	–	–	0.85
2,5-Dimethyl-1,4-benzenodiol	($C_8H_{10}O_2$)	3.11	–	–
2,4-Dimethoxytoluene	($C_9H_{12}O_2$)	–	–	1.27
2,3-Dimethoxytoluene	($C_9H_{12}O_2$)	0.88	–	–
3,4-Dimethoxytoluene	($C_9H_{12}O_2$)	–	0.92	
3,4-Dimethoxyphenol	($C_8H_{10}O_3$)	–	–	0.38
2,6-Dimethoxyphenol	($C_8H_{10}O_3$)	1.19	0.51	–
3,4-Methylenedioxymethoxybenzene	($C_8H_8O_3$)	–	0.29	–
3,5-Dimethoxytoluene	($C_9H_{12}O_2$)	–	–	0.51
2-Methoxy-4-ethyl phenol	($C_9H_{12}O_2$)	–	–	1.84
3-Hydroxy-4-methoxybenzoic acid	($C_9H_{12}O_3$)	5.75	–	–
1,2,4-Trimethoxybenzene	($C_9H_{12}O_3$)	1.46	4. 14	2.84
4-Amino-3,5-diethylpyridine	($C_9H_{14}N_2$)	5. 74	–	–
4-Ethenyl-1,2-dimethoxybenzene	($C_{10}H_{12}O_2$)	–	0.59	0.53
5-Methyl-1,2,3-trimethoxybenzene	($C_{10}H_{14}O_3$)	0.86	0.07	0.59
4-Hydroxy-3-methoxy benzoic acid	($C_8H_8O_4$)	–	1.19	–
2-Methoxy-4-propenilbenzene	($C_{10}H_{12}O$)	–	0.58	–
3,4,5-Trimethoxybenzaldehyde	($C_{10}H_{12}O_4$)	0.37	–	–
1,2-Dimethoxy-4-(2-methoxyethenil)benzene	($C_{11}H_{14}O_3$)	0.17	–	–

[a]The %area was calculated for the identified. The unidentified compounds were excluded

(2-methoxy-4-ethylphenol), are possibly formed by the cleavage of the C_α–C_β bond ($E_d = 259.3$ kJ mol^{-1}) favored by increasing pyrolysis temperature [25, 31]. A relative increase in the production of 4-methylguaiacyl was observed with increasing pyrolysis temperature, while 4-ethylguaiacyl was only obtained at 600 °C, indicating that these products obtention is favored with increasing temperature due to a higher E_d of the C_α–C_β bond.

A series of free radical reactions is employed to explain the formation of phenolic compounds. The methoxy group (–OCH_3) is initially cleaved from the aromatic ring to generate radicals that causes a chain reaction. The hydrogen of the methyl radical is then abstracted, producing the phenol, along with the release of a methylene radical (–CH_2). Sequentially, the methylene radical acts as an H^+ donor for the formation of another type of phenol, promoting new free

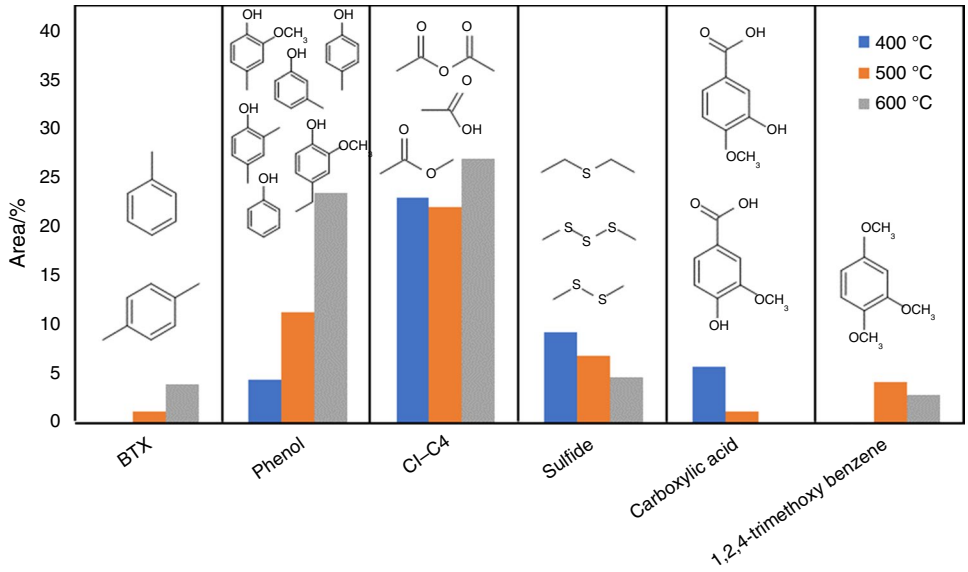

Fig. 9 Main products of kraft lignin pyrolysis

radicals that can be coupled to produce the low molecular weight species, such as CO, CO_2, CH_4 and CH_3OH [25]. In terms of dissociation energy for phenol formation through any mechanism in Fig. 7, the first step is the limiting one thus being energetically feasible the pathway for phenol formation from the decomposition of the primary pyrolytic products [31, 35].

Methyl disulfide, one of the pyrolysis products, is associated with the kraft pulping process due to the use of Na_2S [36]. Other lower molecular mass compounds containing sulfur can be formed through decomposition reactions during pyrolysis, resulting in the formation of SO_x which is not detected by the GC–MS system used in this work.

Kraft lignin has a low volatile content (~46%) and consists mainly of oxygenated and sulfurated compounds, and consequently, this biomass is not the most suitable for biofuel production. However, the content of aromatic compounds (BTEX and phenol) is interesting for the generation of bioproducts precursors indispensable to the industry, such as renewable polymers—substitutes of petroleum-derived plastics—phenolic resins, polyester, adhesives, and dyes.

Figure 10 presents industrial applications of some aromatics that can be obtained through lignin pyrolysis and the relative value-added between them [37]. Among the aromatic compounds illustrated, phenol has the highest value-added.

Aromatic compounds are obtained through technologies that break the lignin structure in monomers without sacrificing the aromatic ring in order to obtain the so-called building block (aromatic monomers such as benzene, xylene, toluene, phenol, and vanillin), considered a fine chemical and largely used by the chemical industry [37].

The use of innovative technologies, such as pyrolysis, has great potential to promote increasingly sustainable processes

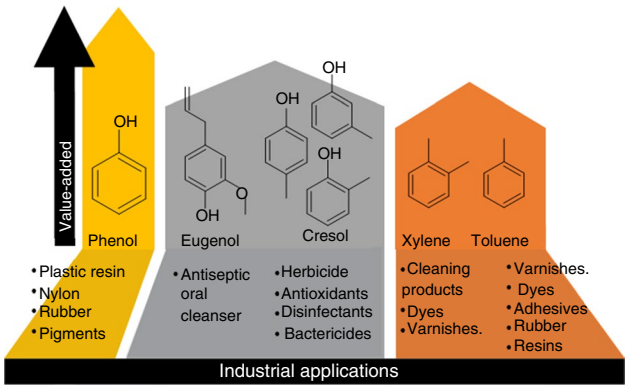

Fig. 10 Applications of aromatics obtained from lignin pyrolysis

and products, as they allow thermally breaking biomass by-product, such as lignin, to produce building blocks that can be used, for example, in the manufacture of 100% biobased PET bottles [38]. In this case, the conventional raw material from a fossil source is completely replaced by raw material from a renewable source.

Conclusions

The low volatiles and high ash content of kraft lignin show a low fuel potential for this material (15 MJ kg^{-1}) when compared to other biomass sources. However, the volatiles produced by pyrolysis at 600 °C showed a composition rich in phenolic compounds, toluene and p-xylene, which can be used as a source of renewable building blocks required by the chemical industry. The kinetic study presented a complex mechanism of lignin degradation, comprising 7 consecutive and parallel reactions. The reaction orders greater than one

for the range 35–840 °C implied a bimolecular degradation mechanism leading to phenol formation, which was one of the main products of the pyrolysis of kraft lignin at 600 °C. Except for the low volatile content, pyrolysis of kraft lignin is a better alternative valorization route to its combustions, which releases CO_2 into the atmosphere, a greenhouse gas. Pyrolysis of kraft lignin can generate precursors of bioproducts of great importance to the industry, such as the development of renewable polymers, replacement of petroleum-based plastics or in the pharmaceutical formulation, phenolic or epoxy resins, polyester, nylons, detergents, membranes, adhesives, and dyes.

Acknowledgements The authors gratefully acknowledge the financial support from National Council for Scientific and Technological Development (CNPq), LABTAM/NUPPRAR/UFRN, for providing facilities and UFMA for providing software's license. This study was financed in part by the CNPq (Project codes: 140525/2020-3 and 307433/2020-0).

Author contributions GO helped in conceptualization, data curation, visualization, formal analysis and writing—original draft. LS contributed to conceptualization, methodology, investigation and writing—original draft. GC, MM and AP were involved in writing—review and editing. DM helped in resources, writing—review and editing. RB performed conceptualization, resources, project administration, supervisor and writing—review and editing.

References

1. Schutyser W, Renders T, Van Den Bosch S, Koelewijn SF, Beckham GT, Sels BF. Chemicals from lignin: an interplay of lignocellulose fractionation, depolymerisation, and upgrading. Chem Soc Rev. 2018. https://doi.org/10.1039/c7cs00566k.
2. Tan SSY, MacFarlane DR, Upfal J, Edye LA, Doherty WOS, Patti AF, Pringle JM, Scott JL. Extraction of lignin from lignocellulose at atmospheric pressure using alkylbenzenesulfonate ionic liquid. Green Chem. 2009. https://doi.org/10.1039/b815310h.
3. IBÁ, Dados Estatísticos. 2020. https://iba.org/dados-estatisticos. Accessed 12 July 2020.
4. Empresa de Pesquisa Energética - EPE, Balanço Energético 2020: Ano Base 2019, Rio de Janeiro, 2020.
5. Hu TQ. Chemical modification, properties, and usage of lignin. 1st ed. New York: Springer; 2002. https://doi.org/10.1007/978-1-4615-0643-0.
6. Vanholme R, Morreel K, Darrah C, Oyarce P, Grabber JH, Ralph J, Boerjan W. Metabolic engineering of novel lignin in biomass crops. New Phytol. 2012. https://doi.org/10.1111/j.1469-8137.2012.04337.x.
7. McKendry P. Energy production from biomass (part 1): overview of biomass. Bioresour Technol. 2002. https://doi.org/10.1016/S0960-8524(01)00118-3.
8. Azadi P, Inderwildi OR, Farnood R, King DA. Liquid fuels, hydrogen and chemicals from lignin: a critical review. Renew Sustain Energy Rev. 2013. https://doi.org/10.1016/j.rser.2012.12.022.
9. Vishtal A, Kraslawski A. Challenges in industrial applications of technical lignins. BioResources. 2011. https://doi.org/10.15376/biores.6.3.vishtal.
10. Rinaldi R, Jastrzebski R, Clough MT, Ralph J, Kennema M, Bruijnincx PCA, Weckhuysen BM. Paving the way for lignin valorisation: recent advances in bioengineering, biorefining and catalysis. Angew Chem Int Ed. 2016. https://doi.org/10.1002/anie.201510351.
11. Liu X, Feng S, Fang Q, Jiang Z, Hu C. Reductive catalytic fractionation of lignin in birch sawdust to monophenolic compounds with high selectivity. Mol Catal. 2020. https://doi.org/10.1016/j.mcat.2020.111164.
12. Naron DR, Collard FX, Tyhoda L, Görgens JF. Influence of impregnated catalyst on the phenols production from pyrolysis of hardwood, softwood, and herbaceous lignins. Ind Crops Prod. 2019. https://doi.org/10.1016/j.indcrop.2019.02.001.
13. Wang W, Luo Z, Li X, Xue S, Sun H. Novel micro-mesoporous composite zsm-5 catalyst for aromatics production by catalytic fast pyrolysis of lignin residues. Catalysts. 2020. https://doi.org/10.3390/catal10040378.
14. Ma Z, Sun Q, Ye J, Yao Q, Zhao C. Study on the thermal degradation behaviors and kinetics of alkali lignin for production of phenolic-rich bio-oil using TGA-FTIR and Py-GC/MS. J Anal Appl Pyrolysis. 2016. https://doi.org/10.1016/j.jaap.2015.12.007.
15. Wang S, Ru B, Lin H, Sun W, Luo Z. Pyrolysis behaviors of four lignin polymers isolated from the same pine wood. Bioresour Technol. 2015. https://doi.org/10.1016/j.biortech.2015.01.127.
16. Liu Q, Wang R, Zheng S, Y, Luo Z, Cen K,. Mechanism study of wood lignin pyrolysis by using TG-FTIR analysis. J Anal Appl Pyrolysis. 2008. https://doi.org/10.1016/j.jaap.2008.03.007.
17. Zhang M, Hu Y, Wang H, Li H, Han X, Eng Y, Xu CC. A review of bio-oil upgrading by catalytic hydrotreatment: advances, challenges, and prospects. Mol Catal. 2021. https://doi.org/10.1016/j.mcat.2021.111438.
18. Cordero T, Marquez F, Rodriguez-Mirasol J, Rodriguez J. Predicting heating values of lignocellulosics and carbonaceous materials from proximate analysis. Fuel. 2001. https://doi.org/10.1016/S0016-2361(01)00034-5.
19. Ozawa T. A new method of analyzing thermogravimetric data. Bull Chem Soc Jpn. 1965. https://doi.org/10.1246/bcsj.38.1881.
20. Flynn JH, Wall LA. General treatment of the thermogravimetry of polymers. J Res Natl Bur Stand Sect A Phys Chem. 1966. https://doi.org/10.6028/jres.070A.043.
21. Khiari B, Jeguirim M, Limousy L, Bennici S. Biomass derived chars for energy applications. Renew Sustain Energy Rev. 2019. https://doi.org/10.1016/j.rser.2019.03.057.
22. Chu S, Subrahmanyam AV, Huber GW. The pyrolysis chemistry of a β-O-4 type oligomeric lignin model compound. Green Chem. 2013. https://doi.org/10.1039/c2gc36332a.
23. Koddenberg T. Handbook of wood chemistry and wood composites. J Clean Prod. 2016. https://doi.org/10.1016/j.jclepro.2015.07.070.
24. Shao L, Zhang X, Chen F, Xu F. Fast pyrolysis of Kraft lignins fractionated by ultrafiltration. J Anal Appl Pyrolysis. 2017. https://doi.org/10.1016/j.jaap.2017.11.003.
25. Shen DK, Gu S, Luo KH, Wang SR, Fang MX. The pyrolytic degradation of wood-derived lignin from pulping process. Bioresour Technol. 2010. https://doi.org/10.1016/j.biortech.2010.02.078.
26. Kawamoto H. Lignin pyrolysis reactions. J Wood Sci. 2017. https://doi.org/10.1007/s10086-016-1606-z.
27. Lin CW, Dence SY. Methods in lignin chemistry. Berlin: Springer; 1992. https://doi.org/10.1007/978-3-642-74065-7.
28. Lou R, Wu S, Lyu G. Quantified monophenols in the bio-oil derived from lignin fast pyrolysis. J Anal Appl Pyrolysis. 2015. https://doi.org/10.1016/j.jaap.2014.12.022.
29. Jiang G, Nowakowski DJ, Bridgwater AV. A systematic study of the kinetics of lignin pyrolysis. Thermochim Acta. 2010. https://doi.org/10.1016/j.tca.2009.10.003.
30. Lu Q, Xie W, Hu B, Liu J, Zhao W, Zhang B, Wang T. A novel interaction mechanism in lignin pyrolysis: phenolics-assisted hydrogen transfer for the decomposition of the β-O-4 linkage.

Combust Flame. 2021;40:5. https://doi.org/10.1016/j.combustflame.2020.11.011.
31. Chen L, Ye X, Luo F, Shao J, Lu Q, Fang Y, Wang X, Chen H. Pyrolysis mechanism of β-O-4 type lignin model dimer. J Anal Appl Pyrolysis. 2015. https://doi.org/10.1016/j.jaap.2015.07.009.
32. Amen-Chen C, Pakdel H, Roy C. Production of monomeric phenols by thermochemical conversion of biomass: a review. Bioresour Technol. 2001. https://doi.org/10.1016/S0960-8524(00)00180-2.
33. Yang C, Lü X. Composition of plant biomass and its impact on pretreatment. In: Lü X, editor. Bioethanol production, 2nd generation. Elsevier; 2021. p. 71–85. https://doi.org/10.1016/B978-0-12-818862-0.00002-9.
34. Asmadi M, Kawamoto H, Saka S. Characteristics of softwood and hardwood pyrolysis in an ampoule reactor. J Anal Appl Pyrolysis. 2017. https://doi.org/10.1016/j.jaap.2017.01.029.
35. Zhang JJ, Jiang XY, Ye XN, Chen L, Lu Q, Wang XH, Dong CQ. Pyrolysis mechanism of a β-O-4 type lignin dimer model compound: a joint theoretical and experimental study. J Therm Anal Calorim. 2016. https://doi.org/10.1007/s10973-015-4944-y.
36. Zhang M, Resende FLP, Moutsoglou A, Raynie DE. Pyrolysis of lignin extracted from prairie cordgrass, aspen, and Kraft lignin by Py-GC/MS and TGA/FTIR. J Anal Appl Pyrolysis. 2012. https://doi.org/10.1016/j.jaap.2012.05.009.
37. Gosselink RJA. Lignin as a renewable aromatic resource for the chemical industry. Wageningen: Wageningen University; 2011.
38. Sudolsky D. Commercializing renewable aromatics for biofuels, biobased chemicals and plastics chemical recycling. Ind Biotechnol. 2019. https://doi.org/10.1089/ind.2019.29192.dsu.